GaN-based High Efficiency Bidirectional DC-DC Converter with 10 MHz Switching Frequency

Kristian Kruse, Mads Elbo and Zhe Zhang
Dept. Electrical Engineering
Technical University of Denmark
Kgs. Lyngby, Denmark
zz@elektro.dtu.dk

***Abstract*—Wide bandgap (WBG) semiconductor devices allow power electronic converters to achieve higher efficiency, higher power density and potentially higher reliability. However, the design challenges accompanied by applying the new WBG devices have risen accordingly. In this paper, a non-isolated bidirectional DC-DC converter equipped with Gallium Nitride (GaN) semiconductor transistors is presented. The converter's operation principles, zero-voltage switching (ZVS) constraints and dead-time effects are studied. Moreover, the optimization and tradeoffs on the adopted high-frequency inductor are investigated. Based on the theoretical analysis and calculation, a laboratory prototype with a switching frequency up to 10 MHz and the maximum output power of 100 W is constructed and tested. Switching at 10 MHz, a power density of approximately 6.25W/cm^3 and an efficiency of 94.4% in the Buck mode are achieved. Moreover, the measured losses can match the theoretically calculated counterparts well, therefore the design and analysis are verified. However, from the experimental test carried out, it can also be seen, that making a compact converter, even for a GaN-based one, operate at 10 MHz and 100 W is still very challenging due to complex ZVS control, lacks of feasible magnetic materials, and limited thermal dissipation area.**

Keywords—Bidirecioinal; converter; DC-DC; dead-time; Gallium Nitride; high switching frequency; soft-switching

I. INTRODUCTION

Bidirectional DC-DC converters, which can effectively interface energy storage devices such as batteries, supercapacitors and reversible fuel cells to power conversion systems within applications of electrical vehicles (EVs), renewable energy generation (REG), uninterruptible power supplies (USPs) etc., have gained increasing attention in academia and industry over the last decade [1]-[3]. Moreover, with the emergence of applying wide bandgap devices such as Silicon Carbide (SiC) and Gallium Nitride (GaN) based power switches, power electronic converters tend to be even faster, smaller and more efficient, due to the increased electrical field strength and electron mobility compared to than their silicon (Si) based counterparts [4]-[9]. A high switching frequency, to some extent, can certainly offer opportunities for converter volume reduction and thereby obtain higher power density and more compact design. However, it is also accompanied by new challenges, for instance, increased switching losses even with wide bandgap devices, worse electromagnetic interference (EMI) and more stress on magnetic components [10], [11].

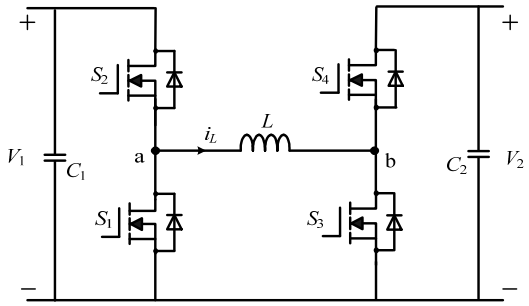

Fig. 1. Topology of the non-inverting Buck-Boost converter

Therefore, soft-switching technologies, including zero-voltage switching (ZVS) and zero-current switching (ZCS), are still widely used in the field of applications of wide band-gap semiconductors. High-frequency soft-switching GaN-based implementations under boundary conduction mode (BCM) have been reported in the literature, in which the reduction of switching loss can well compensate for the increased conduction loss [12]. For instance, a 5-MHz ZVS Boost converter with the efficiency up to 98% was demonstrated in [13]; A ZVS extension method is presented based on synchronous rectification in [14] in which a negative inductor current to discharge the switching node capacitance and can achieve ZVS independently from the converter input to output voltage ratio. In [15], a non-inverting Buck-Boost converter, as shown in Fig. 1, was proposed, and it is able to achieve full ZVS operation, as well as flexible and easy control, which is significantly better than the resonant converters such as Class-E DC-DC converters.

This paper presents a high switching frequency GaN-based bidirectional DC-DC converter which can achieve high efficiency and high power density by a proper design, in particular selecting the optimum dead time. It is shown that the conduction loss increases accordingly when the dead time is longer than the needed ZVS commutation time due to a larger forward voltage drop of GaN devices, thus setting up ideal switching conditions for GaN devices are more severe than their Si counterparts. The paper is organized as follows. After this introduction, the operating principles of the non-inverting bidirectional Buck-Boost converter are given Section II. Then, the ZVS constraints with respect to circuit parameters and the dead time effects on the converter efficiency are discussed in

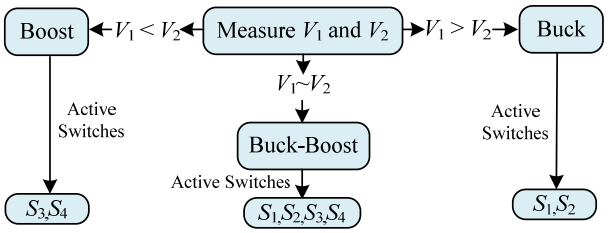

Fig. 2. Equivalent circuits under different operating modes.

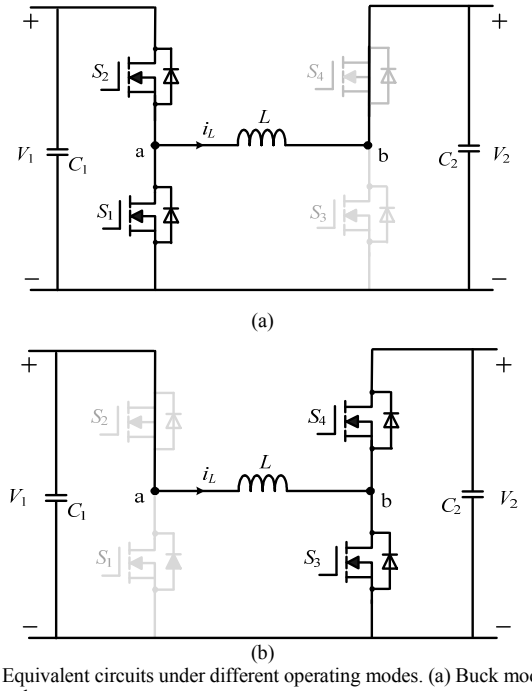

Fig. 3. Equivalent circuits under different operating modes. (a) Buck mode; (b) Boost mode.

Section III. The design and the corresponding laboratory prototype of the GaN-based converter with a switching frequency of 10 MHz are presented in Section IV. Finally, the conclusion is given in Section V.

II. Operation Modes of the Bidirectional Converter

The non-inverting Buck-Boost converter consists of four switches, S_1~S_4 and one inductor L and its topology is depicted in Fig. 1. Basically, the converter can operate in three modes i.e. Buck mode, Boost mode and Buck-Boost mode, depending on the input and output voltage [16], as illustrated in Fig. 2. S_1 and S_2, S_3 and S_4 always have complementary driving signals with a certain dead-time, t_{dd}, respectively, no matter the operating modes. In the Buck mode, S_1 and S_2 are regulated by a duty cycle, and S_3 and S_4 do not operate at the switching frequency, as illustrated in Fig. 3 (a). The low side MOSFET S_1 works as a synchronous rectifier and can achieve soft switching, nevertheless, the high side one S_2 is hard switched. On the other hand, as shown in Fig.3 (b), during the Boost mode, S_3 and S_4 operate at the switching frequency and adjusting their duty cycle can convert the voltage between V_1 and V_2. S_4 turns on under zero voltage. When the voltages V_1

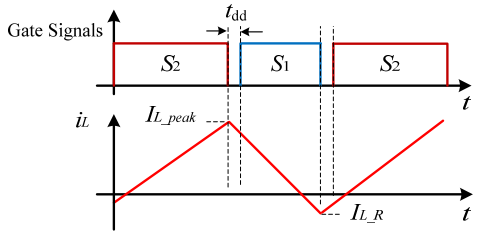

Fig. 4. Typical waveforms of zero-voltage operation.

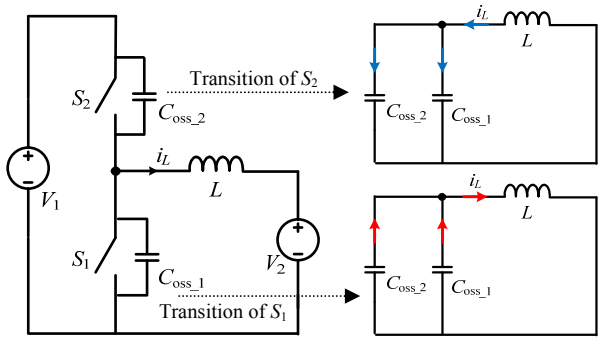

Fig. 5. Zero voltage commutation between high side and low side switches.

and V_2 are very close to each other, the converter must work in the Buck-Boost mode in order to avoid the duty cycle too close to either 1 or zero, which means the Buck-Boost mode is a short transition period between Buck and Boost modes to ensure the smooth and efficient operation within the entire input and output voltage range. Switches S_1 and S_4, as well as S_2 and S_3, turn ON and OFF simultaneously. S_2 and S_3 are soft switched, but the other two switches suffer from turn-on switching loss.

III. Zero-Voltage Switching Constraints and Deadtime Effects

Due to the superior switching performance of wide bandgap devices, adopting them in power converters is accordingly able to reduce switching losses. However, switching losses will still limit the maximum allowed switching frequency within MHz range even for GaN- or SiC-based converters. Moreover, without soft switching, the fast transitions during commutation can cause severe EMI issues which result in rather large filters needed and therefore a bulky and lossy converter. The mechanism for achieving zero-voltage turn-on is, before the switch is triggered, to completely discharge its output capacitance, which means its anti-paralleled or body diode conducts and thereby can clamp the voltage to almost zero in most cases.

The analysis is given based on the Buck operation. However, the same principles can apply to Boost mode and Buck-Boost mode as well. As the waveforms illustrated in Fig. 4, at t_2, the low side switch S_1 is turned OFF, and in order to discharge C_{oss_2} to zero voltage, the inductor current must be reversed or negative, as the equivalent circuits illustrated in Fig. 5. Moreover, the energy stored in the inductor at the commutating moment must satisfy:

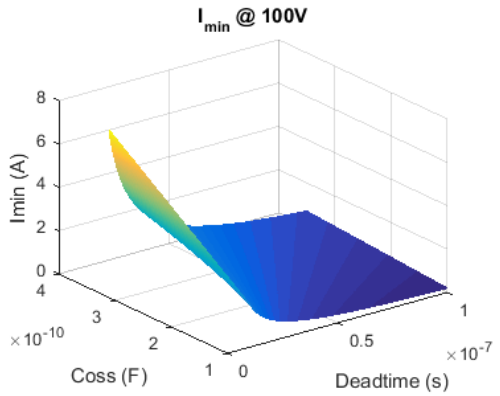

Fig. 6. Minimum I_{L_R} as a function of output capacitance and dead time.

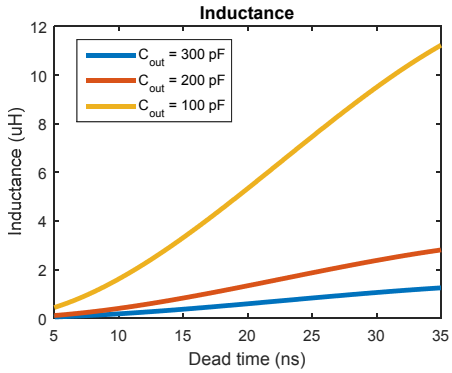

Fig. 7. Inductance needed as a function of dead time at V_1=100 V.

$$E_L \geq \frac{1}{2} C_{oss\_1} \cdot V_{DS\_1}^2 + \frac{1}{2} C_{oss\_2} \cdot V_{DS\_2}^2 \ . \tag{1}$$

where E_L, C_{oss_i}, $_{i=1,2}$, and V_{DS_i}, $_{i=1,2}$ represent energy stored in the inductor L, output capacitance of the switches, and voltage across the switches, respectively.

After the output capacitances C_{oss_1} and C_{oss_2} are fully charged and discharged respectively, the body diodes start to conduct and clamp the drain-to-source voltage. Therefore, the inductor current as expressed in (2) has to be smaller than zero before S_2 is triggered, where t_{dd} is the dead-time.

$$I_L = \frac{\Delta V_L \cdot t_{dd}}{L} = \frac{(V_1 - V_2) \cdot t_{dd}}{L} \ . \tag{2}$$

From (1) and (2), the minimum dead time needed in the Buck mode can be calculated in (3).

$$t_{dd\_\min\_Buck} = \sqrt{\frac{C_{oss\_in\_total} \cdot L \cdot V_1}{(V_1 - V_2)}} \tag{3}$$

where $C_{oss\_in\_total} = C_{oss\_1} + C_{oss\_2}$.

The magitude (absolute value) of the minimum reversed inductor current I_{L_R} as a function of the output capacitance and the dead time is plotted in Fig. 6 with V_1=100 V. It is clear that for a certain dead-time selected, the larger output capacitance is, the larger I_{L_R} is needed. On the other hand, the

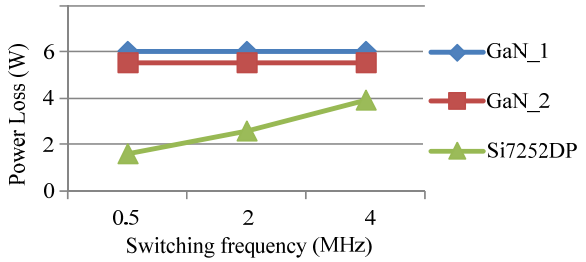

Fig. 8. Reverse conduction loss comparison of Si and GaN devices.

inductance for achieving ZVS can be calculated and plotted in Fig. 7 for different total output capacitance of the half bridge consisting of S_1 and S_2.

Similarly, the minimum dead time needed in the Boost mode and Buck-Boost mode can be expressed by (4) and (5), respectively, where $C_{oss\_out\_total} = C_{oss\_3} + C_{oss\_4}$.

$$t_{dd\_\min\_Boost} = \sqrt{\frac{C_{oss\_out\_total} \cdot L \cdot V_2}{(V_2 - V_1)}} \tag{4}$$

$$t_{dd\_\min\_Buck-Boost} = \sqrt{\frac{(C_{oss\_in\_total} \cdot V_1 + C_{oss\_out\_total} \cdot V_2) \cdot L}{2 \cdot |V_2 - V_1|}} \tag{5}$$

The upper limit of the dead time is determined by the conduction losses allowed when the body diode conducts. Compared to the Si devices, under the same rated block voltage, GaN power transistors have a larger forward voltage drop (3rd quadrant conduction drop). Therefore, Si MOSFET Si7252DP is used as a reference and compared to two different GaN transistors GaN_1 and GaN_2, and the calculated losses are plotted in Fig. 8. It can be seen that, due to the lower forward voltage of the MOSFET, its reverse conduction loss is lower, but the total loss including reverse recovery loss increases as the switching frequency increases. Thus, a precise dead-time control to avoid GaN device reverse conduction is crucial for minimizing losses. However, it is not practical to have such circuit at high switching frequency i.e. 10 MHz.

IV. Experimental Results

To validate the given analysis and design, a 100 W GaN-based non-inverting bidirectional DC-DC converter with a switching frequency of 10 MHz has been built and tested. The specifications used for the converter hardware are listed in Table I.

TABLE I. Specifications

Parameters	*Values*
Voltage of V_1	30-60 VDC
Voltage of V_2	30-60 VDC
Maximum output power, P_o	100 W
Maximum switching frequency, f_s	10 MHz
Inductance, L	120 nH

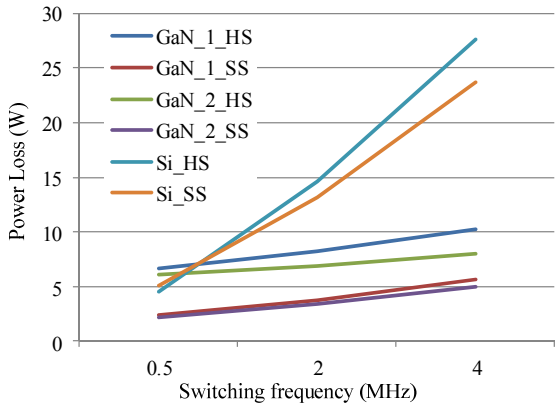

Fig. 9. Total loss comparison of Si and GaN devices.

In order to select GaN devices which can be adopted in this design, two candidates are compared with Si7252DP, with respect to losses, including conduction and switching losses under both soft-switching and hard-switching operation. The losses are calculated under the condition: input voltage of 50V, average current of 2.5 A, RMS current of 3.53 A, current at turn-off of 5 A, and duty cycle of 50%, and the results are plotted in Fig. 9. It is noted that the GaN devices maintain low losses at increased frequencies, compared with the Si device. Taking the gate driver complexity into consideration, eventually, GaN_1 i.e. LMG5200 is applied to the laboratory prototype.

Using Fig. 7, the inductance can be set to 120 *n*H, in order to be able to operate the converter at 10 MHz with the maximum dead time corresponding to 10 % of the total period i.e.10 *n*s. In order for the inductor to uphold a current density of 5 A/mm^2 as well as have a low DC resistance, there will be a number of conductors in parallel. At such a high frequency, AC resistance is mainly due to the skin effect expressed in (6) and (7), where r_w and δ represent winding radius and skin depth, respectively.

$$R_{AC} = k_s \cdot R_{DC} \tag{6}$$

where

$$R_{AC} = 0.25 + 0.5 \cdot \frac{r_w}{\delta} + \frac{3}{32} \cdot \frac{r_w}{\delta} \quad for \quad \frac{r_w}{\delta} > 1.7. \tag{7}$$

The skin effect at 10 MHz gives a depth of 0.021 mm. By using a thin wire of Ø0.04mm the additional losses caused by the AC resistance is reduced drastically. Finally, a solenoid air core inductor with 3 turns and 15mm diameter is made and tested. At 10 MHz, its inductance and resistance are measured as126 *n*H and 101 *m*Ω.

The photograph of the constructed laboratory prototype is shown in Fig. 10. At the output power of 100 W, the thermal distribution is observed by a FLIR thermal imaging camera and presented in Fig. 11. It can be seen that with a small heat sink fixed on its top the case temperature of LMG5200 is as high as 96.5 °C, and thereby extra cooling must be added in order to ensure a reliable operation.

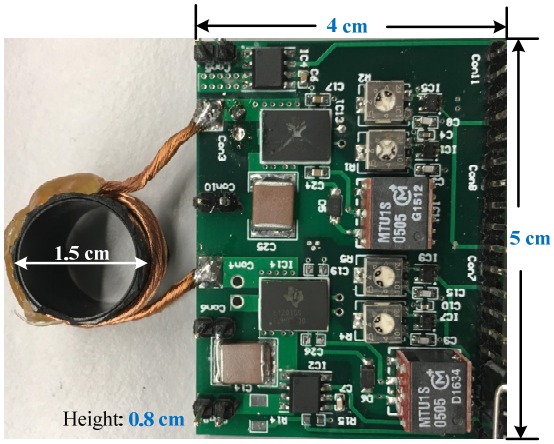

Fig. 10. Photograph of the constructed prototype.

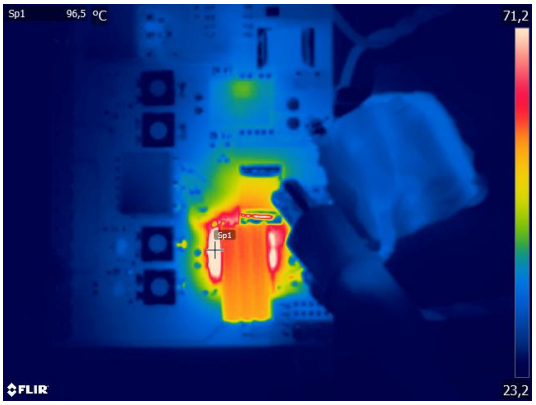

Fig. 11. Photograph of the constructed prototype.

Experimental waveforms captured from the converter are given in Fig. 12. There is a 40 *n*s propagation delay from the gate signal to the gate-to-source voltage. The dead time is minimized in Fig. 12 (a) so that no voltage overshoot or ringing exits over the switch, and thereby the converter efficiency can be improved. Nevertheless, if the dead time is longer than the minimum value, the GaN device start to conduct reversely. As shown in Fig. 12 (b), v_{DS} is clamped at about -3 V, resulting in higher conduction loss. On the other hand, if the dead time is insufficient, the switch cannot operate under complete ZVS, resulting in the associated voltage overshoot and ringing and higher switching loss as illustrated clearly in Fig. 12. (c).

The power efficiency is measured by PPA1530 Precision Power Analyzer in the Buck and Boost modes, and the measured efficiency curves are plotted in Fig. 13. In the Buck mode, V_1=60 V, V_2=30V, and f_s=10 MHz, and the maximum efficiency is 94.4%. In the Boost mode, V_1=40 V, V_2=60 V, and due to non-minimum dead time and the consequence high thermal stress on GaN devices, the switching frequency has to be reduced to 8 MHz, and moreover, when f_s=9 MHz and at 100W the efficiency achieved is 92.9% and only 0.5% lower than that of 8 MHz operation at the same output power.

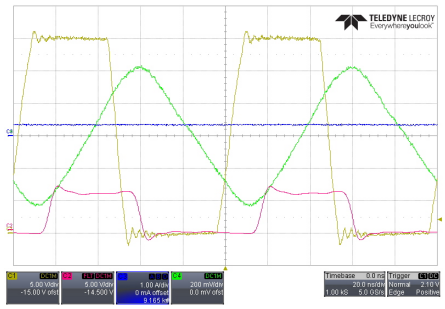

(a)

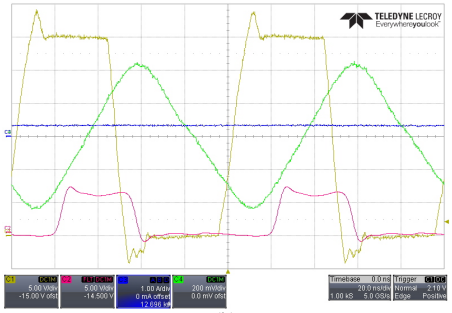

(b)

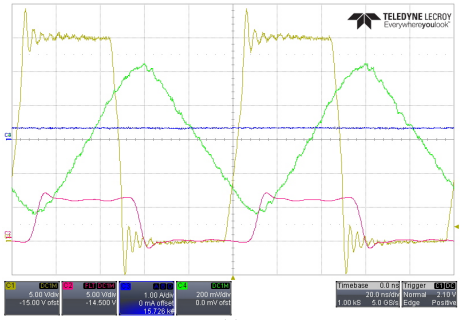

(c)

Fig. 12. Experimental waveforms at 10 MHz. (a) Minimized dead time, (b) GaN reverse conduction and (c) insufficient dead time. CH1: v_{DS_S1}, drain-to-source voltage of S_1; CH2: v_{GS_S1}, gate signal with a 40 *n*s propagation delay; CH3: i_{out}, output DC current; CH4: i_L, inductor current (AC coupling).

V. Conclusion

In this paper, a high-frequency non-inverting Buck-Boost converter equipped with GaN devices is analysed and designed. This converter is able to work in Buck, Boost and Buck-Boost modes depending on input and output voltages, therefore can achieve bidirectional operation. At the switching frequency of 10 MHz, the designed converter can achieve 94.4% efficiency, and the power density is 6.25W/cm^3. A precise dead time control to minimize the conduction loss is important for efficiency improvement. Moreover, operating a GaN-based converter at 10 MHz and output power of 100 W is still a very challenging task due to the limited thermal dissipation area. The embedded gate drivers suffer from high temperature and can be damaged even though in theory GaN transistors can sustain high junction temperatures compared to Si devices. Therefore, in order to increase efficiency as well as power density further, lowering the switching frequency to 4-6

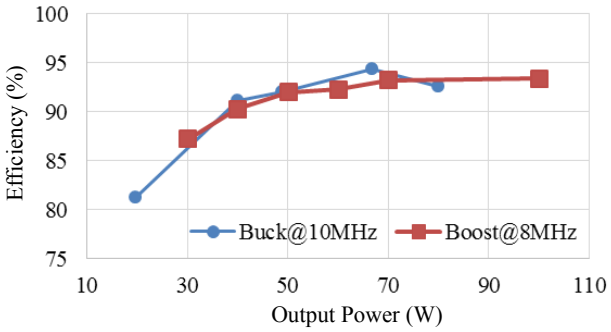

Fig. 13. Measured efficiency.

MHz is preferable, and inductors with magnetic cores instead of air core inductors are then available for an even more compact implementation. Finally, a tradeoff between power density and switching frequency should be carried out in the future to obtain the optimal design for GaN-based power electronic converters.

References

[1] Z. Zhang, O. C. Thomsen and M. A. Andersen, "Optimal design of a push-pull-forward half-bridge (PPFHB) bidirectional DC–DC converter with variable input voltage," *IEEE Transactions on Industrial Electronics*, vol.59, no.7, pp.2761-771, Aug. 2012.

[2] S. Inoue and H. Akagi, "A bidirectional DC-DC converter for an energy storage system with galvanic isolation", *IEEE Transactions on Power Electronics*, vol. 22, no. 6, pp. 2299-2306, Jun. 2007.

[3] T. Konjedic, L. Korosec, C. Restrepo, M. Rodic and M. Milanovic, "DCM-based zero-voltage switching control of a bidirectional DC–DC converter with variable switching frequency," *IEEE Transactions on Power Electronics*, vol. 31, no. 4, pp. 3273-3288, April. 2016.

[4] A. Anthon; Z. Zhang; M. A. E. Andersen; G. Holmes; B. McGrath; C. A. Teixeira, "The benefits of SiC MOSFETs in a T-Type inverter for grid-tie applications," *IEEE Transactions on Power Electronics*, vol.PP, no.99, pp.1-1.

[5] O. Khan, W. Xiao and H. H. Zeineldin, "Gallium-nitride-based submodule integrated converters for high efficiency distributed maximum power point tracking PV applications," *IEEE Transactions on Industrial Electronics*, vol.63, no.2, pp.966-975, Feb. 2016.

[6] S. Waffler, M. Preindl and J. W. Kolar, "Multi-objective optimization and comparative evaluation of Si soft-switched and SiC hard-switched automotive DC-DC converters," *2009 35th Annual Conference of IEEE Industrial Electronics (IECON)*, pp. 3814-3821.

[7] B. Zhao, Q. Song and W. Liu, "Experimental comparison of isolated bidirectional DC–DC converters based on all-Si and all-SiC power devices for next-generation power conversion application," IEEE *Transactions Industrial Electronics*, vol.61, no.3, pp.1389-1393, Mar. 2014.

[8] R. Ramachandran and M. Nymand, "A 98.8% efficient bidirectional full-bridge isolated DC-DC GaN converter," in *Proceedings of IEEE Applied Power Electronics Conference and Exposition (APEC)*. p. 609-614, 2016.

[9] A. Anthon, J. C. Hernandez, Z. Zhang and M. A. E. Andersen, "Switching investigations on a SiC MOSFET in a TO-247 package," in *Proc. IECON*, pp. 1854-1860, 2014.

[10] J. W. Kolar, D. Bortis and D. Neumayr, "A ideal switch is not enough," *Proceedings of the 28th IEEE International Symposium on Power Semiconductor Devices and ICs (ISPSD)*, Jun. 2016.

[11] Y. Han, G. Cheung, A. Li, C. R. Sullivan and D. J. Perreault, "Evaluation of magnetic materials for very high frequency power applications," *IEEE Transactions on Power Electronics*, vol.27, no.1, pp.425-435, Jan. 2012.

[12] X. Huang, Z. Liu, Q. Li, and F. C. Lee, "Evaluation and application of 600 V GaN HEMT in cascode Structure," *IEEE Transactions on Power Electronics*, vol. 29, no. 5, pp. 2453–2461, May 2014.

[13] X. Huang, Z. Liu, F. C. Lee, and Q. Li, "Characterization and enhancement of high voltage cascode GaN devices," *IEEE Transactions on Electron Devices*, vol. 62, no. 2, pp. 270–277, Feb. 2015.

[14] B. Su, J. Zhang, and Z. Lu, "Totem-pole boost bridgeless PFC rectifier with simple zero-current detection and full-range ZVS operating at the boundary of DCM/CCM," *IEEE Transactions on Power Electronics*, vol. 26, no. 2, pp. 427–435, Feb. 2011.

[15] P. Vinciarelli, "Buck-boost DC-DC switching power conversion," U.S. Patent 6,788,033, 2004.

[16] Z. Yu, H. Kaples, and K. H. Hoffmann, "High efficiency bidirectional dc-dc converter with wide input and output voltage ranges for battery systems," *PCIM Europe*, 2015.